Oxidation-induced spin reorientation in Co adatoms and CoPd dimers on Ni/Cu(100)

K. Chen,[1,2] T. Beeck,[1] S. Fiedler,[1] I. Baev,[1] W. Wurth,[1,3] and M. Martins[1]
[1]*Institut für Experimentalphysik, Universität Hamburg, Luruper Chaussee 149, 22761 Hamburg, Germany*
[2]*Synchrotron SOLEIL, L'orme des Merisiers, Saint-Aubin - BP48, 91192 GIF-sur-YVETTE CEDEX, France*
[3]*DESY Photon Science, Notkestraße 85, 22607 Hamburg, Germany*
(Received 7 April 2016; published 27 April 2016)

Ultrasmall magnetic clusters and adatoms are of strong current interest because of their possible use in future technological applications. Here, we demonstrate that the magnetic coupling between the adsorbates and the substrate can be significantly changed through oxidation. The magnetic properties of Co adatoms and CoPd dimers deposited on a remanently magnetized Ni/Cu(100) substrate have been investigated by x-ray absorption and x-ray magnetic circular dichroism spectroscopy at the Co $L_{2,3}$ edges. Using spectral differences, pure and oxidized components are distinguished, and their respective magnetic moments are determined. The Co adatoms and the CoPd dimers are coupled ferromagnetically to the substrate, while their oxides, Co-O and CoPd-O, are coupled antiferromagnetically to the substrate. Along with the spin reorientation from the pure to the oxidized state, the magnetic moment of the adatom is highly reduced from Co to Co-O. In contrast, the magnetic moment of the dimer is of similar order for CoPd and CoPd-O.

DOI: 10.1103/PhysRevB.93.144421

I. INTRODUCTION

The magnetic properties of low-dimensional systems, like atoms, magnetic molecules, nanoparticles, and thin films [1–4] have been an area of particular interest in recent years. There, enhanced magnetic moments and magnetic anisotropy energies per atom can be found due to low-coordination numbers and specific symmetry directions, showing their high potential for magnetic applications. In addition to the reduction in size, alloying of high-spin 3*d* with strong spin-orbit coupling 4*d* and 5*d* transition metals is a promising strategy to stabilize the magnetic moment to a specific direction on the surface [5,6].

How the oxidation influences the magnetic properties is of crucial interest from a fundamental as well as applied point of view and has been studied intensively over the past decade. For example, enhanced orbital-to-spin magnetic moments were found for deposited, oxide covered Co nanoparticles due to uncompensated moments at the Co/CoO interface [7–9]. A large effective additional anisotropy was reported for similar Co core, CoO shell nanoparticles if embedded into an antiferromagnetic CoO matrix [10]. A similar important role of the exchange bias effect was addressed to exchange coupled magnetic molecules deposited on magnetic 3*d* substrates [11,12]. If the magnetic molecules are separated from the substrate by an oxygen layer, the coupling switches from ferro- to antiferromagnetic.

In order to understand these findings in more detail, small, mass selected clusters are excellent systems as they are large enough to show complex phenomena and small enough to be treated with sophisticated theoretical methods. In recent work, magnetic moments as a function of the number of atoms per cluster have been studied for 3*d* and rare earth elements [13–19]. In addition to the strong size dependence, the magnetic moments of the clusters are sensitively influenced by the chemical environment [20–22]. For example, CoPt alloy clusters can be easily oxidized even under UHV conditions. The oxidation results in a significant decrease of the magnetization [19].

In this paper, Co adatoms and CoPd dimers deposited on a remanently magnetized Ni/Cu(100) substrate are investigated by means of x-ray absorption (XAS) and x-ray magnetic circular dichroism (XMCD) spectroscopy at the Co $L_{2,3}$ edges, respectively. Thus, the chemical state and the magnetic property of the Co atom for each sample is determined. Oxidation of all Co adatoms and almost half of the CoPd dimers is achieved by a modification of the preparation procedure.

II. EXPERIMENT

The ability of XMCD to determine spin and orbital magnetic moments in an element specific way makes it the favorable method to study magnetic properties of deposited clusters. The Co atoms and the CoPd dimers are produced by high energy ion sputtering using 30 keV Xe^+ ions to erode the target material and thereby produce the clusters. To mass select Co and CoPd from the various clusters sizes, the beam is deflected by a magnetic dipole field with a resolution of $m/\Delta m \approx 50$. The production and mass separation of the clusters is carried out at a base pressure of 2×10^{-8} mbar. Figure 1(a) shows the mass spectra of the clusters up to Co_4 produced from the CoPd target. As a result of the sputtering process, Xe^+ ions are also present in the mass spectrum. A more detailed description of the cluster source and its capabilities was given previously [23].

In the deposition process, the clusters are refocused and decelerated down to a kinetic energy of about 1 eV/atom to reduce fragmentation and implantation into the substrate. In addition, a soft landing scheme [24,25] is used, where Kr condensed onto the sample surface is used as a buffer system. Thus, fragmentation of the clusters is suppressed effectively [26,27]. The Kr is desorbed by flash heating to $\sim$ 120 K before the measurements. Hence, the clusters are directly supported by the substrate surface as illustrated in Fig. 1(b). Low sample temperatures ($\sim$ 30 K) are used to inhibit cluster agglomeration and therefore, in combination with a low coverage of about 0.03 monolayers, cluster-cluster interaction can be neglected in our samples. The 20 monolayer thin Ni films have been prepared on the clean Cu(100) substrate

 ©2016 American Physical Society

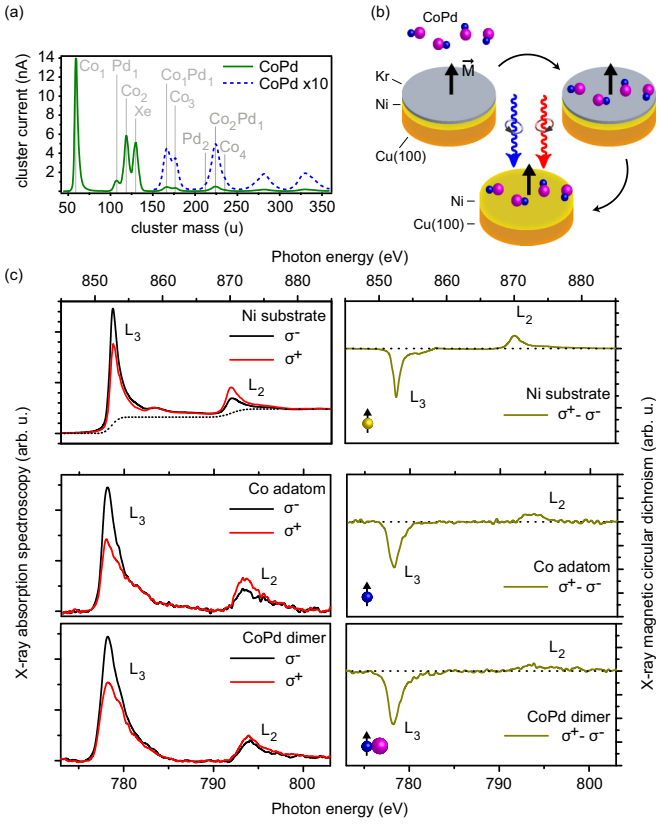

FIG. 1. (a) Mass spectrum of Co and CoPd alloy cluster ions produced from the CoPd target. (b) Sketch for the soft landing procedure used for the clusters. (c) (From top to bottom) X-ray absorption and magnetic dichroism spectroscopy for the Ni film (top axis), the Co adatoms, and the CoPd dimers (bottom axis), respectively. The same negative signal at the Ni and Co L_3 edge indicates parallel spin moments of the Co adatom, the CoPd dimer, and the Ni film.

and are remanently magnetized perpendicular to the surface by short pulses from a small solenoid. The layer thickness has been calibrated and monitored by the XAS intensity ratio of the Ni and Cu $L_{2,3}$ edges.

All measurements have been carried out at a base pressure below 5×10^{-10} mbar. As a measure for the XAS spectra of the adsorbates, the total electron yield (TEY), in our experiment the total sample current, is recorded. The experiments have been carried out at beamline UE52-SGM [28] with a constant degree of 90% circular polarization at the BESSY II storage ring in Berlin. All samples have been prepared *in situ* at the synchrotron. XMCD spectra have been taken at the Ni and Co $L_{2,3}$ edges with a counting time of 4*s* per data point for each photon helicity. The beamline resolution for the Co $2p$-$3d$ spectra is 200 meV [28]; so was the step width we set for the spectra.

III. RESULTS AND DISCUSSION

XAS and XMCD spectra for the Ni film, the Co adatoms, and the CoPd dimers are shown in Fig. 1(c). The Co and the CoPd XAS spectra show no characteristic oxidation multiplets, known from CoO bulk, nanoparticles, and clusters [19,29–31]. Similar to the Co atom, the CoPd dimer is ferromagnetically coupled to the out of plane magnetized Ni/Cu(001) substrate as can be seen from the same negative XMCD signal at the Co and Ni L_3 edge.

Deposited Co atoms and CoPd dimers are very stable against oxidation, as the XAS does not change during the measurements over hours. Therefore, some activation energy is needed to oxidize both species. However, during the soft landing process the ions are landed in the rare gas matrix with a kinetic energy of about 1eV/atom. Consequently, the atoms and dimers are rather hot which could promote the oxidation process if oxygen is present on the substrate. The latter is naturally given by a very small amount of adsorbed residual gas (mainly H_2O, CO, CO_2) at 30 K. Surprisingly, a correlation between the amount of the adsorbed residual gas, defined by the time τ_w between the preparation of the magnetized Ni film and the adsorption of the Kr buffer gas layer, and the oxidation of the Co and CoPd samples was found as will be shown in the following. However, the oxidation process itself remains unclear.

Figure 2(a) shows how the XAS spectra change if τ_w is increased from < 5 min. (Co, CoPd) to 60 min ($CoPd_{ox.}$) and 90 min (Co-O). With increased τ_w, a multiplet structure emerges that is common for CoO [19,29–31]. Along with the appearance of the multiplet structures in the XAS, the corresponding XMCD signal shown in Fig. 2(b) is modified.

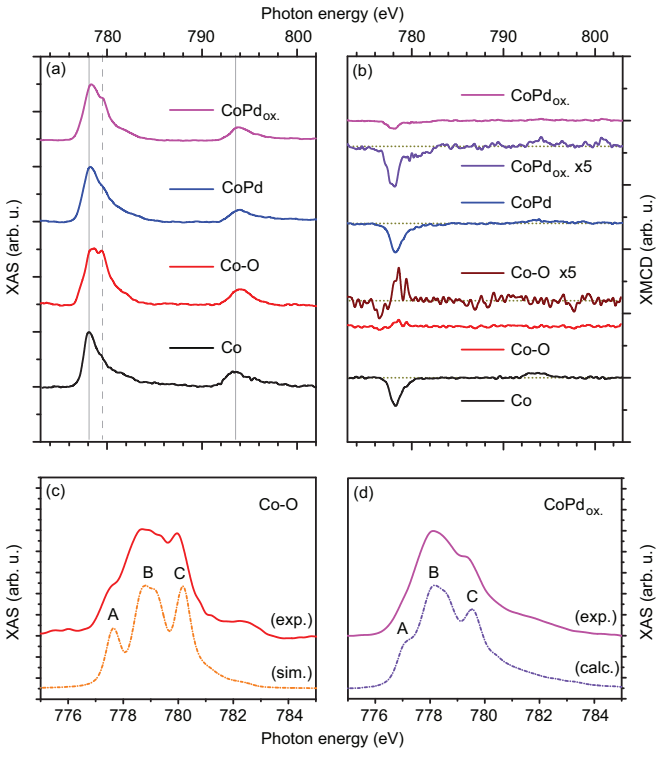

FIG. 2. (a) L-edge XAS and (b) XMCD spectra of Co, Co-O, CoPd and $CoPd_{ox.}$ adatoms (from bottom to top), respectively. Along with the appearance of the multiplet structures in the XAS of Co-O and $CoPd_{ox.}$, the XMCD signal is reduced. (c) and (d) Comparison of the XAS of Co-O and $CoPd_{ox.}$, using the simulated Co^{2+} spectra from CTM4XAS only (Co-O) and, calculated by linear combination, together with the experimental CoPd XAS spectrum, respectively.

For oxidized Co adatoms, marked as Co-O in the following, the XMCD signal at the L_3 edge is rather small (about 1/5 of the Co adatom) and reverts to positive indicating antiparallel coupling to the Ni film. For the oxidized CoPd sample, preliminary marked as $CoPd_{ox.}$, the XMCD signal at the L_3 edge is also small (1/5 of the CoPd cluster) but stays negative. Thus, parallel coupling to the Ni film is indicated.

As sketched in Fig. 2(c), the XAS of Co-O is in good agreement with simulated Co^{2+} spectra obtained from CTM4XAS [32] using ligand field multiplet (LFM) calculations based on Cowan's atomic structure code [33]. The calculation was performed for $Co^{2+}(3d^7)$ in cubic crystal field (O_h) symmetry with 10Dq = 1.1 eV, corresponding to a high-spin state [21,34]. The Slater integrals were scaled to 0.75 of their atomic values to account for solid state effects. The overall good agreement in the energy positions and the relative heights of the multiplet features between the calculated multiplet spectrum and the experimental spectrum shows that the Co-O sample is almost fully oxidized. The magnetization of Co-O is small and in particular antiparallel to the spin moments of the Ni film. Thus, a spin reorientation in the Co atom is induced by the oxidation. The situation is more complex for the $CoPd_{ox.}$ sample since it looks like the CoPd spectra but with an additional shoulder peak 1.5 eV above the L_3 edge. Hence, the $CoPd_{ox.}$ spectrum can be interpreted as an ensemble of unoxidized CoPd and oxidized CoPd-O dimers on the substrate. If, in a simple approach, the oxidized CoPd-O dimers are considered to exhibit a similar charge state as for Co-O (Co^{2+}), the $CoPd_{ox.}$ spectrum can be calculated by a linear combination of the simulated LFM spectrum and the experimental spectrum of the unoxidized CoPd. A comparison of the relative multiplet peak heights [marked A, B, and C in Figs. 2(d) and 3(a)] allows us to determine the contribution of both species. The XAS spectra of $CoPd_{ox.}$ can be fitted with $60 \pm 5\%$ CoPd and $40 \pm 5\%$ CoPd-O spectra and therefore, is labeled CoPd-$O_{0.4}$ in the following. Due to the high magnetization of the CoPd dimer parallel to the Ni moment, the small and also parallel net magnetization of the CoPd-$O_{0.4}$ sample indicates a strong negative contribution from the CoPd-O components.

The experimental and the calculated XAS of the CoPd-$O_{0.4}$ sample are given in Fig. 3(a) as an example how the spectrum can be decomposed into two fractions of 60% CoPd and 40% CoPd-O. In a similar fashion, the magnetic contribution of CoPd-O can be derived by subtracting the contribution of CoPd from the XMCD spectra of CoPd-$O_{0.4}$, as is shown in Fig. 3(b). In Fig. 3(d), the resulting XMCD spectrum of the extrapolated CoPd-O is presented. While the magnetic moment of the CoPd dimer couples parallel to the Ni, the coupling is antiparallel for CoPd-O [see also illustration in Fig. 3(c)]. Compared to the small antiparallel moment of the Co-O adatoms, the opposite moment for CoPd-O is of comparable size to the CoPd dimers. Like for the Co adatom, a spin reorientation of the CoPd dimer from parallel to antiparallel to the Ni is induced by oxidation. Note that within 60 min only 40% of the CoPd dimers are oxidized while the Co adatoms are almost fully oxidized 90 min after the Ni preparation. Thus, the oxidation rate for Co and CoPd is different.

To confirm the antiparallel coupling between the CoPd-O and the Ni film, two further preparations with $\tau_w = 5$, 20 min (CoPd-$O_{0.05}$ and CoPd-$O_{0.25}$) were produced and measured. Figure 4(a) shows how the multiplet structure emerges from CoPd to CoPd-$O_{0.4}$, indicating a stronger CoPd-O contribution. As expected, the total XMCD signal shown in Fig. 4(b) is decreasing due to the stronger contribution of CoPd-O.

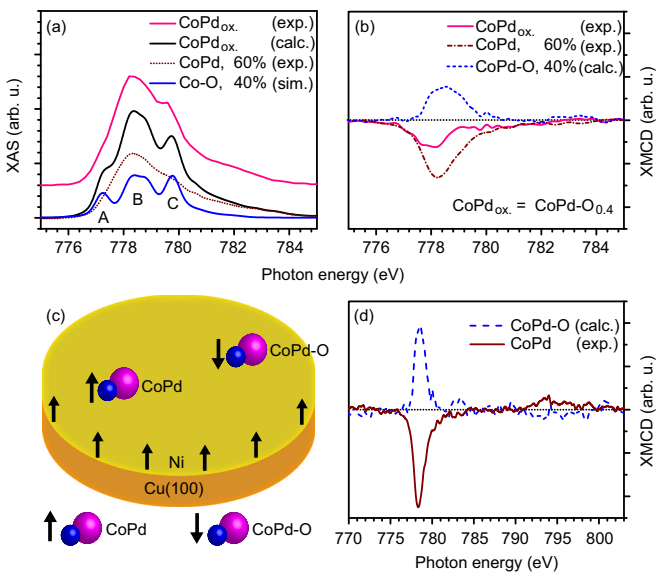

FIG. 3. The XAS (a) and XMCD (b) spectra of $CoPd_{ox.}$ together with the components from CoPd (60%) and CoPd-O (40%). Note that the labeling is changed from $CoPd_{ox.}$ to CoPd-$O_{0.4}$ due to the latter contribution. (c) Sketch for the parallel and antiparallel magnetization alignment of CoPd and CoPd-O in the $CoPd_{ox.}$ sample. (d) Normalized XMCD for CoPd and CoPd-O adatoms.

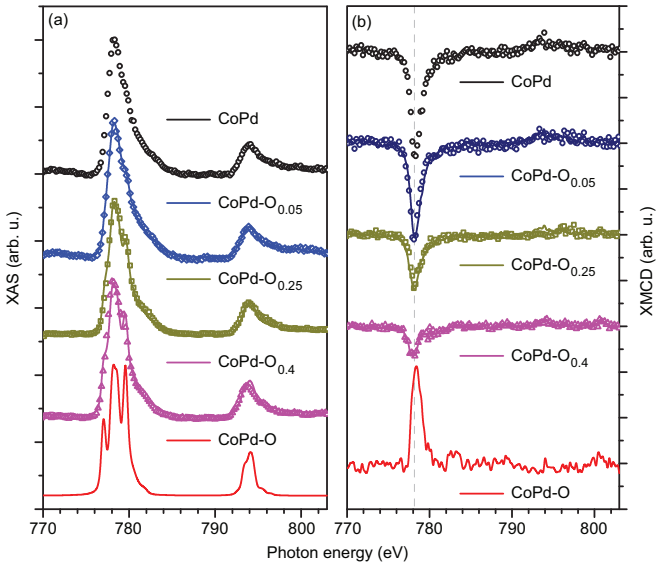

FIG. 4. $L_{2,3}$ edge XAS (a) and XMCD (b) of different CoPd preparations with changing oxidation rate. The circles resemble experimental data while the solid lines are calculated. From the latter, the oxidation rate of the samples CoPd-$O_{0.05}$, CoPd-$O_{0.25}$, and CoPd-$O_{0.40}$ are derived to be 5%, 25%, and 40%, respectively. At the bottom, CoPd-O XAS (simulated by LFM) and XMCD (calculated by linear combination) spectra are shown.

TABLE I. The evaluated spin (m_S), orbital (m_L), and total ($m_S + m_L$) magnetic moments for Co and CoPd adatoms in μ_B/d-hole are shown together with the ratio m_L/m_S. Except CoPd-O, all magnetic moments result from experimental spectra.

Cluster	$m_L + m_S$	m_S	m_L	m_L/m_S
Co	0.57 ± 0.09	0.45 ± 0.06	0.12 ± 0.03	0.27 ± 0.06
CoPd	0.64 ± 0.10	0.46 ± 0.06	0.18 ± 0.04	0.39 ± 0.06
CoPd-$O_{0.05}$	0.58 ± 0.09	0.42 ± 0.05	0.16 ± 0.04	0.39 ± 0.06
CoPd-$O_{0.25}$	0.33 ± 0.06	0.24 ± 0.03	0.09 ± 0.03	0.38 ± 0.06
CoPd-$O_{0.40}$	0.17 ± 0.04	0.12 ± 0.02	0.05 ± 0.02	0.37 ± 0.06
Co-O	−0.04 ± 0.02	−0.03 ± 0.01	−0.01 ± 0.005	0.34 ± 0.11
CoPd-O	−0.40 ± 0.14	−0.29 ± 0.09	−0.11 ± 0.04	0.38 ± 0.11

By using the same fitting procedure as described earlier for CoPd-$O_{0.4}$, the CoPd-O contribution of the additional samples were determined. The oxidation rates for CoPd-$O_{0.05}$ and CoPd-$O_{0.25}$ are $5 \pm 5\%$ and $25 \pm 5\%$, respectively, as already indicated by the indices. From the derived sample compositions, the experimental XMCD signals were fitted [Fig. 4(b), solid lines]. The calculated spectra fit nicely the experimental data.

The well-known sum rules [35–37] allow us to determine the effective spin magnetic moment m_S^{eff}, the orbital magnetic moment m_L, and the orbital to spin ratio m_L/m_S^{eff} from the XMCD spectra. The effective spin magnetic moment, $m_S^{\text{eff}} = m_S + 7m_t$, consists of the spin magnetic moment m_S and the magnetic dipole moment m_t. The latter accounts for the asphericity of the spin moment distribution and cannot be neglected in cluster systems [38]. In the following, we will refer to m_S^{eff} as an effective spin moment denoted for simplicity as m_S. The evaluated magnetic moments are shown in Table I and Fig. 5 in units of μ_B/d-hole. Note that except of CoPd-O, all moments are evaluated directly from the experimental data.

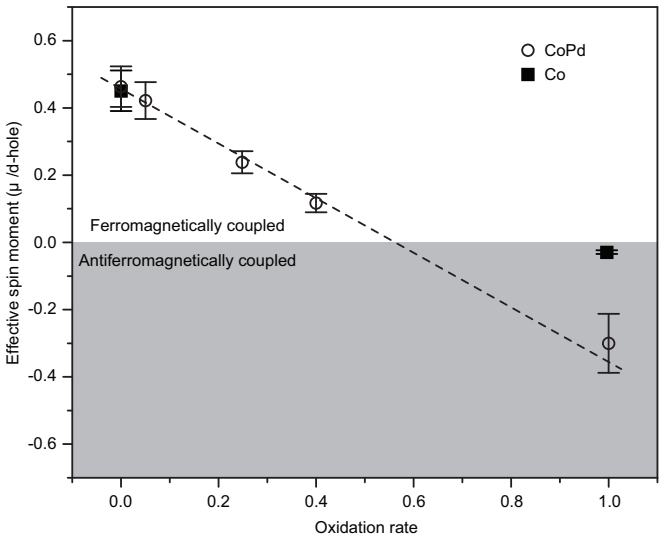

FIG. 5. The effective magnetic spin moment m_S^{eff} for the Co and CoPd dimer is plotted in dependence to the oxidation rate. The negative values of Co-O and CoPd-O indicate an antiparallel coupling to the Ni substrate. The moment of CoPd-O is obtained by a linear extrapolation, as discussed in the text.

The value for the Co adatom is in good agreement with earlier measurements [19]. For CoPd, the spin moment is similar to the Co atom while the orbital moment is about 35% enhanced. Thus, the orbital to spin ratio increases by 30%. If the oxidation ratio of the CoPd dimers increases, the spin and orbital moments are decreasing linearly, as indicated for the spin moment in Fig. 5. Consequently, the orbital to spin ratio is almost constant and independent of the oxidation ratio. The negative sign for Co-O and CoPd-O describes the antiparallel coupling of the Co moments relative to the Ni. Compared to the Co adatom the total magnetic moment of Co-O is almost quenched from 0.57 to −0.04. In contrast, the total moment of CoPd-O is reduced only by 40% with respect to the CoPd. Alloying Co and Co-O with Pd has diverse influence on the orbital and spin magnetic moment. While alloying of a Co adatom with Pd shows relatively moderate changes of the magnetic moments, both the orbital and spin magnetic moment are remarkably enhanced by one order if a Pd atom is added to Co-O.

IV. CONCLUSIONS

In this paper, we have shown how the magnetic moments of a Co adatom and a CoPd dimer on Ni/Cu(100) are influenced by oxidation. Samples with different oxidation rates have been prepared by setting the time between the preparation of the Ni film and the deposition of the adsorbates. Unfortunately, the mechanism behind the oxidation process remains unclear. The XMCD spectra show an oxidation induced spin reorientation for Co-O on Ni/Cu(100). Samples with increased oxidation ratios exhibit reduced dichroism thus, a similar reorientation for CoPd-O is reasonable. Co and CoPd are ferromagnetically coupled while Co-O and CoPd-O are antiferromagnetically coupled with respect to the Ni film. Whereas the magnetic moment of Co-O is almost quenched, the extrapolated moment of CoPd-O is reduced only by 40% with respect to CoPd. Remarkably, the CoPd-O orbital and spin magnetic moments increase by one order if a Pd atom is added to Co-O.

ACKNOWLEDGMENTS

The work was supported by the Deutsche Forschungsgemeinschaft DFG via the SFB668 project A7. The experimental support from BESSY beamline staff is grateful acknowledged.

[1] I. G. Rau, S. Baumann, S. Rusponi, F. Donati, S. Stepanow, L. Gragnaniello, J. Dreiser, C. Piamonteze, F. Nolting, S. Gangopadhyay, O. R. Albertini, R. M. Macfarlane, C. P. Lutz, B. A. Jones, P. Gambardella, A. J. Heinrich, and H. Brune, Science **344**, 988 (2014).

[2] M. Mannini, F. Pineider, P. Sainctavit, C. Danieli, E. Otero, C. Sciancalepore, A. M. Talarico, M.-A. Arrio, A. Cornia, D. Gatteschi, and R. Sessoli, Nat. Mater. **8**, 194 (2009).

[3] J. Bansmann, A. Kleibert, M. Getzlaff, A. F. Rodriguez, F. Nolting, C. Boeglin, and K.-H. Meiwes-Broer, Phys. Status Solidi B **247**, 1152 (2010).

[4] O. Šipr, S. Bornemann, H. Ebert, S. Mankovsky, J. Vackář, and J. Minár, Phys. Rev. B **88**, 064411 (2013).

[5] P. Gambardella, S. Rusponi, M. Veronese, S. S. Dhesi, C. Grazioli, A. Dallmeyer, I. Cabria, R. Zeller, P. H. Dederichs, K. Kern, C. Carbone, and H. Brune, Science **300**, 1130 (2003).

[6] J. H. Mokkath, J. Magn. Magn. Mater. **349**, 109 (2014).

[7] C. F. J. Flipse, C. B. Rouwelaar, and F. M. F. de Groot, Eur. Phys. J. D **9**, 479 (1999).

[8] U. Wiedwald, M. Spasova, E. L. Salabas, M. Ulmeanu, M. Farle, Z. Frait, A. Fraile Rodriguez, D. Arvanitis, N. S. Sobal, M. Hilgendorff, and M. Giersig, Phys. Rev. B **68**, 064424 (2003).

[9] G. Chuan-Nan, W. Xian-Gang, E. Pellegrin, H. Zhi-Wei, W.-I. Liang, M. Bruns, Z. Wen-Qin, and D. You-Wei, Chin. Phys. B **24**, 034501 (2015).

[10] V. Skumryev, S. Stoyanov, Y. Zhang, G. Hadjipanayis, D. Givord, and J. Nogus, Nature (London) **423**, 850 (2003).

[11] M. Bernien, J. Miguel, C. Weis, Md. E. Ali, J. Kurde, B. Krumme, P. M. Panchmatia, B. Sanyal, M. Piantek, P. Srivastava, K. Baberschke, P. M. Oppeneer, O. Eriksson, W. Kuch, and H. Wende, Phys. Rev. Lett. **102**, 047202 (2009).

[12] D. Chylarecka, C. Wäckerlin, T. K. Kim, K. Müller, F. Nolting, A. Kleibert, N. Ballav, and T. A. Jung, J. Phys. Chem. Lett. **1**, 1408 (2010).

[13] J. T. Lau, A. Föhlisch, R. Nietubyc, M. Reif, and W. Wurth, Phys. Rev. Lett. **89**, 057201 (2002).

[14] J. T. Lau, A. Föhlisch, M. Martins, R. Nietubyc, M. Reif, and W. Wurth, New J. Phys. **4**, 98 (2002).

[15] M. Reif, L. Glaser, M. Martins, and W. Wurth, Phys. Rev. B **72**, 155405 (2005).

[16] M. Martins, M. Reif, L. Glaser, and W. Wurth, Eur. Phys. J. D **45**, 539 (2007).

[17] S. Lounis, M. Reif, P. Mavropoulos, L. Glaser, P. Dederichs, M. Martins, S. Blügel, and W. Wurth, Eur. Phys. Lett. **81**, 47004 (2008).

[18] K. Chen, S. Fiedler, I. Baev, T. Beeck, W. Wurth, and M. Martins, New J. Phys. **14**, 123005 (2012).

[19] L. Glaser, K. Chen, S. Fiedler, M. Wellhöfer, W. Wurth, and M. Martins, Phys. Rev. B **86**, 075435 (2012).

[20] J.-Y. Kim, J.-H. Park, B.-G. Park, H.-J. Noh, S.-J. Oh, J. S. Yang, D.-H. Kim, S. D. Bu, T.-W. Noh, H.-J. Lin, H.-H. Hsieh, and C. T. Chen, Phys. Rev. Lett. **90**, 017401 (2003).

[21] Y. J. Lee, M. P. de Jong, and R. Jansen, Appl. Phys. Lett. **96**, 082506 (2010).

[22] V. R. Singh, K. Ishigami, V. K. Verma, G. Shibata, Y. Yamazaki, T. Kataoka, A. Fujimori, F.-H. Chang, D.-J. Huang, H.-J. Lin, C. T. Chen, Y. Yamada, T. Fukumura, and M. Kawasaki, Appl. Phys. Lett. **100**, 242404 (2012).

[23] J. T. Lau, A. Achleitner, H.-U. Ehrke, U. Langenbuch, M. Reif, and W. Wurth, Rev. Sci. Instrum. **76**, 063902 (2005).

[24] J. T. Lau, A. Achleitner, and W. Wurth, Chem. Phys. Lett. **317**, 269 (2000).

[25] J. T. Lau, W. Wurth, H.-U. Ehrke, and A. Achleitner, Low Temp. Phys. **29**, 223 (2003).

[26] H. Cheng and U. Landman, Science **260**, 1304 (1993).

[27] S. Fedrigo, W. Harbich, and J. Buttet, Phys. Rev. B **58**, 7428 (1998).

[28] F. Senf, F. Eggenstein, U. Flechsig, R. Follath, S. Hartlaub, H. Lammert, T. Noll, J. S. Schmidt, G. Reichardt, O. Schwarzkopf, M. Weiss, T. Zeschke, and W. Gudat, Nucl. Instrum. Methods Phys. Res., Sect. A **467-468**, 474 (2001).

[29] F. M. F. de Groot, M. Abbate, J. van Elp, G. A. Sawatzky, Y. J. Ma, C. T. Chen, and F. Sette, J. Phys.: Condens. Matter **5**, 2277 (1993).

[30] T. J. Regan, H. Ohldag, C. Stamm, F. Nolting, J. Lüning, J. Stöhr, and R. L. White, Phys. Rev. B **64**, 214422 (2001).

[31] P. Imperia, L. Glaser, M. Martins, P. Andreazza, J. Penuelas, V. Alesandrovic, H. Weller, C. Andreazza-Vignolle, and W. Wurth, Phys. Status Solidi A **205**, 1047 (2008).

[32] E. Stavitski, F. M. F. de Groot, Micron **41**, 687 (2010).

[33] R. D. Cowan, *The Theory of the Atomic Structure and Spectra* (University of California Press, Berkeley, 1981); P. H. Butler, *Point Group Symmetry Applications: Methods and Tables* (Plenum, New York, 1981).

[34] H. Ikeno, F. M. F. de Groot, E. Stavitski, and I. Tanaka, J. Phys.: Condens. Matter **21**, 104208 (2009).

[35] B. T. Thole, P. Carra, F. Sette, and G. van der Laan, Phys. Rev. Lett. **68**, 1943 (1992).

[36] P. Carra, B. T. Thole, M. Altarelli, and X. Wang, Phys. Rev. Lett. **70**, 694 (1993).

[37] C. T. Chen, Y. U. Idzerda, H. J. Lin, N. V. Smith, G. Meigs, E. Chaban, G. H. Ho, E. Pellegrin, and F. Sette, Phys. Rev. Lett. **75**, 152 (1995).

[38] O. Šipr, J. Minár, and H. Ebert, Europhys. Lett. **87**, 67007 (2009).